*Chemical Science International Journal*

***20(3): 1-10, 2017; Article no.CSIJ.36656***
***ISSN: 2456-706X***
*(Past name: American Chemical Science Journal, Past ISSN: 2249-0205)*

# Structural and Thermal Studies on Racemic $BaC_4H_4O_6 \cdot H_2O$

**Takanori Fukami[1*], Seiya Hiyajyo[1] and Shuta Tahara[1]**

*[1]Department of Physics and Earth Sciences, Faculty of Science, University of the Ryukyus, Okinawa 903-0213, Japan.*

***Authors' contributions***

*This work was carried out in collaboration between all authors. Author TF performed measurements, managed the literature searches, and wrote the first draft of the manuscript. Authors SH and ST revised the manuscript and participated in group discussions. All authors have read and approved the final manuscript.*

***Article Information***

DOI: 10.9734/CSJI/2017/36656
Editor(s):
(1) Pradip K. Bhowmik, Department of Chemistry, University of Nevada Las Vegas, USA.
Reviewers:
(1) Yongchun zhu, Shenyang Normal University, China.
(2) Paulo T. C., Freire, Universidade Regional do Cariri, Brazil.
Complete Peer review History: http://www.sciencedomain.org/review-history/21267

***Original Research Article***

***Received 6th September 2017***
***Accepted 1st October 2017***
***Published 6th October 2017***

## ABSTRACT

Single crystals of racemic barium tartrate monohydrate, $BaC_4H_4O_6 \cdot H_2O$, were grown at 308 K by a gel method using silica gel as the growth medium. Differential scanning calorimetry, thermogravimetric-differential thermal analysis, and X-ray diffraction measurements were performed on the single crystals. The space group symmetry (monoclinic $P2_1/c$) and structural parameters were determined at room temperature. The crystal structure consisted of $BaO_9$ and $BaO_{10}$ polyhedra, two independent $C_4H_4O_6$ molecules, and O–H···O and C–H···O hydrogen bonds between adjacent $H_2O$ or $C_4H_4O_6$ molecules. Weight losses due to thermal decomposition of racemic $BaC_4H_4O_6 \cdot H_2O$ were found to occur in the temperature range of 300–1550 K. We suggested that the weight losses were caused by the evaporation of bound water molecules and the evolution of $H_2CO$, $H_2$, CO, and $O_2$ gases from the two $C_4H_4O_6$ molecules, and that the residual chalky white and black substances that remained as a mixture in the vessel after decomposition were barium oxide (BaO) and barium monocarbide (BaC), respectively.

**Corresponding author: E-mail: fukami@sci.u-ryukyu.ac.jp;*

*Keywords: Racemic $BaC_4H_4O_6{\cdot}H_2O$; crystal structure; thermal decomposition; TG-DTA; X-ray diffraction.*

## 1. INTRODUCTION

Many tartrate compounds are formed by reacting tartaric acid (chemical formula: $C_4H_6O_6$; systematic name: 2,3-dihydroxybutanedioic acid) with compounds containing positive ions (two monovalent cations or one divalent cation) [1–6]. Tartaric acid has two chiral carbon atoms in its structure, which provides the possibility for four possible different forms of chiral, racemic, and achiral isomers: L(+)-tartaric, D(–)-tartaric, racemic (DL-) tartaric, and meso-tartaric acid [6–8]. Some of these compounds are of interest due to their physical properties, particularly their excellent dielectric, ferroelectric, piezoelectric, and nonlinear optical properties [1,9–11]. Moreover, they are used in numerous industrial applications, for example, as transducers and in linear and non-linear mechanical devices [1,4,11].

Silgo et al. have published the crystal structure of barium L-tartrate, $BaC_4H_4O_6$, as determined at room temperature by means of single-crystal X-ray diffraction [12]. The crystal structure was orthorhombic with space group $P2_12_12_1$, and consisted of $BaO_9$ polyhedra, $C_4H_4O_6$ molecules, and O–H···O hydrogen bonds between adjacent molecules. The positions of hydrogen atoms were calculated based on geometric criteria (O–H and C–H distances of 0.82 and 0.98 Å, respectively), and the atoms were refined with fixed positional and isotropic displacement parameters. Recently, we have determined a more accurate crystal structure in which the positional and thermal parameters of all the atoms including hydrogen atoms were refined, and reported the existence of zig-zag hydrogen-bonded chains along the *a*- and *c*-axes linked by O–H···O and C–H···O hydrogen bonds between adjacent $C_4H_4O_6$ molecules [5]. Moreover, the chemical reactions occurring during the thermal decomposition of L-$BaC_4H_4O_6$ in the temperature range of 450–1530 K were found to be:

$$BaC_4H_4O_6 \rightarrow BaC_4O_6 + 2H_2$$
$$BaC_4O_6 \rightarrow BaC_2O_4 + 2CO$$
$$BaC_2O_4 \rightarrow BaCO_3 + CO$$
$$BaCO_3 \rightarrow BaCO_2 + (1/2)O_2$$
$$BaCO_2 \rightarrow BaC + O_2.$$

Thus, the weight losses due to the thermal decomposition were confirmed to be caused by the evolution of $H_2$, CO, and $O_2$ gases, and the resulting black substance in the vessel after decomposition was barium monocarbide BaC [5].

DL-tartaric compounds have been synthesized with divalent cations by using DL-tartaric acid as a crystallization reagent instead of L(+)-tartaric acid [2,13]. We have grown single crystals of racemic calcium tartrate tetrahydrate, DL-$CaC_4H_4O_6{\cdot}4H_2O$, by the gel method and have determined the crystal structure at room temperature (triclinic with space group $P\bar{1}$) [13]. Moreover, it was found that a phase transition derived from intramolecular proton transfer between three possible sites occurred at around 310 K. The chemical reactions during the thermal decomposition of DL-$CaC_4H_4O_6{\cdot}4H_2O$ were found to be:

$$CaC_4H_4O_6{\cdot}4H_2O \rightarrow CaC_4H_4O_6 + 4H_2O$$
$$CaC_4H_4O_6 \rightarrow CaC_2O_4 + 2H_2CO$$
$$CaC_2O_4 \rightarrow CaC_2O_3 + (1/2)O_2$$
$$CaC_2O_3 \rightarrow CaO + 2CO.$$

Moreover, single crystals of racemic strontium tartrate tetrahydrate, DL-$SrC_4H_4O_6{\cdot}4H_2O$, were also grown by the gel method, and their structural and thermal properties were found to be very similar to those of DL-calcium tartrate [14]. However, investigations of the crystal growth and physical properties of DL-tartaric compounds other than those of DL-$CaC_4H_4O_6{\cdot}4H_2O$ and DL-$SrC_4H_4O_6{\cdot}4H_2O$ have not been carried out yet [13,14].

As mentioned above, it is expected that a racemic barium tartrate compound can be synthesized using a $Ba^{2+}$ ion as a divalent cation and DL-tartaric acid. In this paper, we report the synthesis of single crystals of racemic barium tartrate monohydrate, $BaC_4H_4O_6{\cdot}H_2O$, using the gel method, and determine their crystal structure at room temperature using X-ray diffraction. Moreover, the thermal properties of the DL-barium salt are studied by means of differential scanning calorimetry (DSC) and thermogravimetric-differential thermal analysis (TG-DTA).

## 2. EXPERIMENTAL

### 2.1 Crystal Growth

Single crystals of DL-$BaC_4H_4O_6{\cdot}H_2O$ were grown in a silica gel medium at 308 K using the single

test tube diffusion method. The gels were prepared in test tubes (length of 200 mm, and diameter of 30 mm) using aqueous solutions of $Na_2SiO_3$ (25 ml of 1 M), DL-$C_4H_6O_6$ (25 ml of 1 M), and $CH_3COOH$ (25 ml of 1 M), and aged for six days. A solution of $Ba(NO_3)_2$ (30 ml of 0.25 M) was then gently poured on top of the gel, and the test tubes containing the gel and solution were placed in a drying apparatus kept at the constant temperature of 308 K by a temperature control unit. The crystals were harvested after six months. Samples used for measurements were cut from transparent areas on the tips of the crystals.

## 2.2 Structure Determination

The X-ray diffraction measurements were carried out using a Rigaku Saturn CCD X-ray diffractometer with graphite-monochromated Mo $K_\alpha$ radiation ($\lambda$ = 0.71073 Å). The diffraction data were collected at 299 K using an $\omega$ scan mode with a crystal-to-detector distance of 40 mm, and processed using the CrystalClear software package. The intensity data were corrected for Lorentz polarization and absorption effects. The structure was solved by direct methods using the SIR2011 program and refined on $F^2$ by full-matrix least-squares methods using the SHELXL-2013 program in the WinGX package [15–17].

## 2.3 Thermal Measurements

DSC and TG-DTA measurements were carried out in the temperature ranges of 100–490 K and 300–1550 K, respectively, using DSC7020 and TG-DTA7300 systems from Seiko Instruments Inc. Aluminium (for DSC) and platinum (for TG-DTA) open pans with no pan cover were used as measuring vessels and reference pans. Fine powder samples, prepared by grinding some transparent areas of the crystals, were used for the measurements. The sample amount varied between 3.02 and 5.22 mg, and the heating rates were 5 or 10 K $min^{-1}$ under a dry nitrogen gas flow.

# 3. RESULTS AND DISCUSSION

## 3.1 Crystal Structure

The crystal structure of DL-$BaC_4H_4O_6{\cdot}H_2O$ was determined by the single-crystal X-ray diffraction method at room temperature. The lattice parameters calculated from all observed reflections showed that the crystal belongs to the monoclinic system. The intensity statistics and systematic extinctions of the observed reflections revealed that the crystal structure has a centric space group of $P2_1/c$. Thus, the space group of DL-$BaC_4H_4O_6{\cdot}H_2O$ was determined to be

**Table 1. Crystal data, intensity data collection, and structure refinement for DL-$BaC_4H_4O_6{\cdot}H_2O$**

| | |
|---|---|
| Compound, $M_r$ | $BaO_7C_4H_6$, 303.42 |
| Crystal color | Colorless |
| Measurement temperature | 299 K |
| Crystal system, space group | Monoclinic, $P2_1/c$ |
| Lattice constants | $a$ = 9.3805(3) Å, $b$ = 7.8957(3) Å, $c$ = 19.0742(7) Å, $\beta$ = 91.202(1)° |
| $V$, $Z$ | 1412.43(9) $Å^3$, 8 |
| $D$(cal.), $\mu$(Mo $K_\alpha$), $F$(000) | 2.854 Mg $m^{-3}$, 5.623 $mm^{-1}$, 1136 |
| Crystal size | 0.14×0.26×0.30 mm |
| $\theta$ range for data collection | 2.14–38.00° |
| Index ranges | $-15 \le h \le 15$, $-13 \le k \le 13$, $-32 \le l \le 32$ |
| Reflections collected, unique | 39522, 7446 [$R$(int) = 0.0330] |
| Completeness to $\theta_{max}$ | 96.7 % |
| Absorption correction type | Numerical |
| Transmission factor $T_{min}$–$T_{max}$ | 0.2647–0.4996 |
| Date, parameter | 6669 [$I > 2\sigma(I)$], 266 |
| Final $R$ indices | $R_1$ = 0.0288, $wR_2$ = 0.0498 |
| $R$ indices (all data) | $R_1$ = 0.0355, $wR_2$ = 0.0531 |
| Weighting scheme | $w = 1/[\sigma^2(F_o^2)+(0.016P)^2+1.257P]$ $P = (F_o^2+2F_c^2)/3$ |
| Goodness-of-fit on $F^2$ | 1.162 |
| Extinction coefficient | 0.0015(1) |
| Largest diff. peak and hole | 1.916 and -1.556 e$Å^{-3}$ |

monoclinic $P2_1/c$ with cell parameters $a$ = 9.3805(3) Å, $b$ = 7.8957(3) Å, $c$ = 19.0742(7) Å, and $\beta$ = 91.202(1)°. The atomic coordinates and thermal parameters of all the atoms including hydrogen atoms were refined. A final $R$-factor of 2.88 % was calculated for 6669 unique observed reflections. The relevant crystal data, and a summary of the intensity data collection and structure refinement parameters are given in Table 1. Fig. 1 shows a projected view of the DL-$BaC_4H_4O_6{\cdot}H_2O$ crystal structure along the $b$-axis. The positional parameters in fractions of the unit cell and the thermal parameters are listed in Table 2. Selected bond lengths and angles are given in Table 3, and the hydrogen-bond geometry is presented in Table 4.

The lattice constants observed along the $a$- and $b$-axes are similar to those previously reported for L-$BaC_4H_4O_6$, but the value of the $c$-axis is approximately twice as large [5]. Thus, the volume of the unit cell (1412.43(9) $Å^3$) is more than twice that of L-$BaC_4H_4O_6$ (621.79(3) $Å^3$). Moreover, the calculated density of 2.854 Mg $m^{-3}$ is lower than that of L-$BaC_4H_4O_6$, which is 3.049 Mg $m^{-3}$. Eight water molecules are present in the unit cell of the observed structure, which were taken from the solution used for crystallization, while there are no water molecules in the L-$BaC_4H_4O_6$ crystal [5]. This difference is probably strongly related to the difference in the density. The observed structure of DL-$BaC_4H_4O_6{\cdot}H_2O$ consists of $BaO_9$ and $BaO_{10}$ polyhedra, two independent $C_4H_4O_6$ and $H_2O$ molecules, and O–H···O and C–H···O hydrogen bonds between adjacent $C_4H_4O_6$ or $H_2O$ molecules. Each Ba atom in the unit cell is surrounded by nine or ten O atoms forming $BaO_9$ or $BaO_{10}$ polyhedra, as listed in Table 3. The lengths of the Ba–O bonds are in the range of 2.705(2)–3.128(2) Å, and the average Ba–O distances in the $BaO_9$ and $BaO_{10}$ polyhedra are 2.861 and 2.871 Å, respectively. These values are larger than that of the $BaO_9$ polyhedra in L-$BaC_4H_4O_6$ (2.818 Å) [5]. This is also considered to be related to the difference in the densities of the crystals.

The lengths of twelve O–C bonds in the two independent $C_4H_4O_6$ molecules are in the range of 1.246(2)–1.422(2) Å, as listed in Table 3. The variation in O–C distances is probably related to differences in bond type, as the upper and lower values match the typical lengths of single and double O–C bonds in organic molecules (around 1.43 and 1.22 Å, respectively). Thus, the O(3)–C(2), O(4)–C(3), O(9)–C(6), and O(10)–C(7) bonds on the hydroxyl groups have single-bond character (with lengths of about 1.42 Å), while the remaining eight bonds have double-bond character (with lengths of about 1.25 Å). Moreover, the lengths of six C–C bonds are in the range of 1.523(3)–1.547(3) Å. Since typical C–C single bonds in organic molecules are around 1.54 Å, these six bonds have single-bond character. The angles between the two least-squares planes of atoms in the two $C_4H_4O_6$ molecules, [O(1)O(2)O(3)C(1)C(2) and O(4)O(5) O(6)C(3)C(4)], and [O(7)O(8)O(9)C(5)C(6) and O(10)O(11)O(12)C(7)C(8)], were calculated to be 30.2(1)° and 42.12(8)°, respectively. These calculated angles are much smaller than that of L-$BaC_4H_4O_6$ (67.17(8)°), indicating that the $C_4H_4O_6$ molecules are more planar [5]. Although they do not have completely identical molecular structures due to differences in the occlusal plane angles and in interatomic distances and angles (Table 3), it can be seen that the two independent $C_4H_4O_6$ molecules are related to each other by a mirror plane, and also that the chemically equivalent molecules possessing an inversion center in the unit cell are mirror images of each other. Therefore, it is believed that the $C_4H_4O_6$ molecules in DL-$BaC_4H_4O_6{\cdot}H_2O$ have racemic characters.

The $H_2O$ molecules are interstitially intercalated between the $C_4H_4O_6$ molecules, leaving them at intervals of one-half of the $c$-axis distance, as shown in Fig. 1. The O–H···O and C–H···O hydrogen bonds, which are formed between adjacent $H_2O$ or $C_4H_4O_6$ molecules, build hydrogen-bonding networks in the $bc$-plane. The structures formed by the networks in DL-$BaC_4H_4O_6{\cdot}H_2O$ differ significantly from that formed by the zig-zag hydrogen-bonding networks along the $a$- and $c$-axes in L-$BaC_4H_4O_6$ [5]. The lengths of the O–H···O bonds are in the range of 2.695(2)–3.286(3) Å, while of the C–H···O bonds are in the range of 3.353(2)–3.855(3) Å, as shown in Table 4. The C–H···O bonds are longer than the O–H···O bonds. Thus, the bonding strength of the C–H···O bonds is weaker than that of the O–H···O bonds since the magnitude of bonding strength is mainly reflected in the bond length.

## 3.2 Thermal Analysis

Fig. 2 shows the DTA, TG, and differential TG (DTG) curves of the DL-$BaC_4H_4O_6{\cdot}H_2O$ crystal in the temperature range of 300–1550 K. The sample weight (powder) used for the measurements was 5.22 mg, and the heating rate was 10 K $min^{-1}$ under a nitrogen gas flow of

300 ml $min^{-1}$. The DTA curve exhibits five endothermic peaks at 328.9, 523.3, 733.7, 1062.6, and 1283.3 K, including small peaks. Moreover, eight peaks at 328.4, 527.0, 541.2, 587.4, 632.5, 725.9, 1050.6, and 1276.4 K, including a small shoulder peak, are observed in the DTG curve. These DTA peaks correspond relatively closely to the respective DTG peaks. The DTG curve, which is the first derivative of TG curve, reveals the temperature dependence of the rate of weight loss. Thus, the DTA peaks are associated with the maximum rate of weight loss in the TG curve due to thermal decomposition of the sample.

DSC measurements on the powder sample of DL-$BaC_4H_4O_6{\cdot}H_2O$ were performed in the temperature range from 100 to 490 K at a heating rate of 5 K $min^{-1}$. No obvious endothermic or exothermic peaks were observed in the DSC curve, except for a weak broad endothermic peak at 322.7 K corresponding to that at 328.9 K in the DTA curve. In general, it is believed that a clear peak in DSC curve is attributed to a change in exchange energy at a phase transition. Thus, the obtained results indicate that there is no phase transition in the temperature range of 100–322 K for the DL-$BaC_4H_4O_6{\cdot}H_2O$ crystal.

The TG curve shows the temperature-dependent weight loss of the DL-$BaC_4H_4O_6{\cdot}H_2O$ crystal. After heating the sample up to 1550 K, a mixture of chalky white and black substances was found in the open vessel. In previous papers, we have reported that white oxide products remain

**Table 2. Atomic coordinates and thermal parameters (×$10^4$ Å$^2$) for DL-$BaC_4H_4O_6{\cdot}H_2O$ at room temperature, with standard deviations in brackets. The anisotropic thermal parameters are defined as exp[ $-2\pi^2(U_{11}a^{*2}h^2+U_{22}b^{*2}k^2+U_{33}c^{*2}l^2+2U_{23}b^*c^*kl+2U_{13}a^*c^*hl+2U_{12}a^*b^*hk)$ ]. The isotropic thermal parameters (Å$^2$) for H atoms are listed under $U_{11}$**

| Atom | *X* | *Y* | *Z* | $U_{11}$ | $U_{22}$ | $U_{33}$ | $U_{23}$ | $U_{13}$ | $U_{12}$ |
|---|---|---|---|---|---|---|---|---|---|
| Ba(1) | 0.47015(2) | 0.42311(2) | 0.15686(2) | 185.8(5) | 201.8(6) | 181.9(5) | -16.9(4) | 37.0(4) | -16.1(4) |
| Ba(2) | 0.03597(2) | 0.01576(2) | 0.37406(2) | 159.8(5) | 164.8(5) | 186.7(5) | 3.2(4) | 20.7(3) | 14.8(4) |
| C(1) | 0.8607(2) | 0.6564(3) | 0.2994(1) | 227(8) | 152(8) | 182(8) | 22(6) | -9(6) | -10(6) |
| C(2) | 0.7808(2) | 0.4880(2) | 0.3087(1) | 190(8) | 139(7) | 171(7) | -9(6) | 2(6) | -5(6) |
| C(3) | 0.8140(2) | 0.4175(2) | 0.3825(1) | 156(7) | 133(7) | 171(7) | -7(6) | 21(6) | -3(6) |
| C(4) | 0.7183(2) | 0.2665(2) | 0.3985(1) | 143(7) | 160(8) | 210(8) | 28(6) | 1(6) | -5(6) |
| C(5) | 0.3495(2) | 0.2793(2) | 0.3222(1) | 183(8) | 144(8) | 201(8) | -9(6) | 8(6) | 19(6) |
| C(6) | 0.2848(2) | 0.4560(3) | 0.3291(1) | 156(7) | 163(8) | 205(8) | 16(6) | 47(6) | 19(6) |
| C(7) | 0.3264(2) | 0.5328(2) | 0.4013(1) | 156(7) | 145(8) | 220(8) | 8(6) | 24(6) | 14(6) |
| C(8) | 0.2295(2) | 0.6826(3) | 0.4164(1) | 168(7) | 179(8) | 198(8) | -21(6) | 21(6) | 30(6) |
| O(1) | 0.8185(2) | 0.7781(2) | 0.33543(9) | 296(8) | 154(7) | 343(8) | -52(6) | 6(6) | -3(6) |
| O(2) | 0.9629(2) | 0.6596(2) | 0.25779(9) | 352(9) | 303(9) | 250(7) | 4(6) | 110(7) | -108(7) |
| O(3) | 0.8126(2) | 0.3694(2) | 0.25521(8) | 293(8) | 177(7) | 200(6) | -45(5) | 11(6) | 9(6) |
| O(4) | 0.9588(2) | 0.3644(2) | 0.38705(9) | 147(6) | 168(6) | 298(7) | 1(6) | -8(5) | -14(5) |
| O(5) | 0.7628(2) | 0.1215(2) | 0.3847(1) | 222(7) | 147(7) | 478(10) | -26(7) | 66(7) | -22(5) |
| O(6) | 0.5987(2) | 0.2963(2) | 0.4234(1) | 172(7) | 296(9) | 456(10) | 106(8) | 105(7) | 39(6) |
| O(7) | 0.3009(2) | 0.1666(2) | 0.3617(1) | 236(7) | 164(7) | 404(9) | 63(6) | 46(6) | -18(6) |
| O(8) | 0.4459(2) | 0.2543(2) | 0.27943(9) | 340(9) | 271(8) | 255(7) | 35(6) | 117(6) | 144(7) |
| O(9) | 0.3337(2) | 0.5598(2) | 0.27432(9) | 361(9) | 216(7) | 261(8) | 88(6) | 125(7) | 85(7) |
| O(10) | 0.4697(2) | 0.5877(2) | 0.4030(1) | 144(6) | 207(7) | 435(10) | -35(7) | -7(6) | 29(5) |
| O(11) | 0.2781(2) | 0.8294(2) | 0.41464(9) | 234(7) | 155(6) | 349(8) | 31(6) | 41(6) | 31(5) |
| O(12) | 0.1004(2) | 0.6479(2) | 0.4268(1) | 168(7) | 306(9) | 548(11) | -182(8) | 99(7) | -21(6) |
| O(13) | 0.0955(2) | 0.3458(3) | 0.00649(9) | 267(8) | 318(9) | 249(8) | 47(7) | -1(6) | -37(7) |
| O(14) | 0.3939(2) | 0.3617(4) | 0.0163(1) | 338(10) | 829(18) | 256(9) | -101(11) | -11(8) | 155(11) |
| H(1) | 0.890(4) | 0.329(4) | 0.262(2) | 0.038(9) | | | | | |
| H(2) | 0.002(4) | 0.447(5) | 0.402(2) | 0.06(1) | | | | | |
| H(3) | 0.682(3) | 0.514(3) | 0.306(1) | 0.017(6) | | | | | |
| H(4) | 0.797(3) | 0.501(3) | 0.416(2) | 0.020(7) | | | | | |
| H(5) | 0.276(5) | 0.628(6) | 0.265(2) | 0.07(1) | | | | | |
| H(6) | 0.518(4) | 0.509(5) | 0.408(2) | 0.05(1) | | | | | |
| H(7) | 0.181(3) | 0.439(4) | 0.329(2) | 0.021(7) | | | | | |
| H(8) | 0.312(3) | 0.446(4) | 0.435(2) | 0.025(7) | | | | | |
| H(9) | 0.046(5) | 0.265(6) | 0.016(2) | 0.07(1) | | | | | |
| H(10) | 0.170(4) | 0.328(5) | 0.013(2) | 0.04(1) | | | | | |
| H(11) | 0.371(6) | 0.422(8) | -0.016(3) | 0.16(2) | | | | | |
| H(12) | 0.449(6) | 0.300(7) | -0.001(3) | 0.10(2) | | | | | |

**Table 3. Selected interatomic distances (in Å) and angles (in degrees) for DL-$BaC_4H_4O_6 \cdot H_2O$**

| | | | |
|---|---|---|---|
| Ba(1)–O(1)[1] | 2.946(2) | Ba(1)–O(5)[2] | 2.790(2) |
| Ba(1)–O(7)[2] | 2.909(2) | Ba(1)–O(8)[2] | 2.982(2) |
| Ba(1)–O(8) | 2.705(2) | Ba(1)–O(9) | 2.819(2) |
| Ba(1)–O(10)[1] | 2.943(2) | Ba(1)–O(11)[1] | 2.849(2) |
| Ba(1)–O(14) | 2.802(2) | Ba(1)–C(4)[2] | 3.393(2) |
| Ba(1)–C(5)[2] | 3.302(2) | Ba(2)–O(1)[3] | 2.857(2) |
| Ba(2)–O(2)[1] | 2.760(2) | Ba(2)–O(3)[1] | 3.095(2) |
| Ba(2)–O(4)[4] | 2.858(2) | Ba(2)–O(5)[4] | 2.706(2) |
| Ba(2)–O(7) | 2.771(2) | Ba(2)–O(11)[5] | 2.802(2) |
| Ba(2)–O(12)[5] | 3.128(2) | Ba(2)–O(13)[6] | 2.798(2) |
| Ba(2)–O(13)[7] | 2.938(2) | Ba(2)–C(8)[5] | 3.287(2) |
| O(1)–C(1) | 1.251(3) | O(2)–C(1) | 1.258(3) |
| O(3)–C(2) | 1.421(2) | O(4)–C(3) | 1.422(2) |
| O(5)–C(4) | 1.249(3) | O(6)–C(4) | 1.249(2) |
| O(7)–C(5) | 1.257(2) | O(8)–C(5) | 1.246(2) |
| O(9)–C(6) | 1.412(2) | O(10)–C(7) | 1.413(2) |
| O(11)–C(8) | 1.247(3) | O(12)–C(8) | 1.261(2) |
| C(1)–C(2) | 1.538(3) | C(2)–C(3) | 1.540(3) |
| C(3)–C(4) | 1.528(3) | C(5)–C(6) | 1.528(3) |
| C(6)–C(7) | 1.547(3) | C(7)–C(8) | 1.523(3) |
| O(1)–C(1)–O(2) | 125.9(2) | O(1)–C(1)–C(2) | 116.1(2) |
| O(2)–C(1)–C(2) | 118.0(2) | O(3)–C(2)–C(1) | 112.2(2) |
| O(3)–C(2)–C(3) | 112.1(2) | O(4)–C(3)–C(2) | 109.7(2) |
| O(4)–C(3)–C(4) | 108.8(2) | O(5)–C(4)–O(6) | 124.1(2) |
| O(5)–C(4)–C(3) | 118.2(2) | O(6)–C(4)–C(3) | 117.7(2) |
| O(7)–C(5)–O(8) | 123.9(2) | O(7)–C(5)–C(6) | 116.4(2) |
| O(8)–C(5)–C(6) | 119.7(2) | O(9)–C(6)–C(5) | 109.3(2) |
| O(9)–C(6)–C(7) | 110.6(2) | O(10)–C(7)–C(6) | 111.2(2) |
| O(10)–C(7)–C(8) | 109.3(2) | O(11)–C(8)–O(12) | 124.0(2) |
| O(11)–C(8)–C(7) | 119.8(2) | O(12)–C(8)–C(7) | 116.1(2) |
| C(1)–C(2)–C(3) | 109.2(2) | C(2)–C(3)–C(4) | 110.9(2) |
| C(5)–C(6)–C(7) | 110.0(2) | C(6)–C(7)–C(8) | 109.4(2) |

*(Symmetry codes: (1) -x+1,y-1/2,-z+1/2; (2) -x+1,y+1/2,-z+1/2; (3) x-1,y-1,z; (4) x-1,y,z; (5) x,y-1,z; (6) x,-y+1/2,z+1/2; (7) -x,y-1/2,-z+1/2.)*

**Table 4. Hydrogen bond distances (in Å) and angles (in degrees)**

| D–H···A | D–H | H···A | D···A | <D–H···A |
|---|---|---|---|---|
| O(3)–H(1)···O(2)[1] | 0.80(3) | 1.96(3) | 2.695(2) | 152(3) |
| O(4)–H(2)···O(12)[2] | 0.81(4) | 1.89(4) | 2.704(2) | 174(4) |
| O(9)–H(5)···O(3)[3] | 0.78(5) | 2.11(4) | 2.853(2) | 159(4) |
| O(10)–H(6)···O(6) | 0.78(4) | 1.86(4) | 2.625(2) | 168(4) |
| O(13)–H(9)···O(12)[4] | 0.81(5) | 1.99(4) | 2.745(2) | 153(4) |
| O(13)–H(10)···O(14) | 0.72(4) | 2.12(4) | 2.804(3) | 160(4) |
| O(14)–H(11)···O(7)[5] | 0.80(6) | 2.52(6) | 3.066(3) | 127(5) |
| O(14)–H(11)···O(11)[6] | 0.80(6) | 2.51(6) | 3.286(3) | 162(6) |
| O(14)–H(12)···O(6)[5] | 0.79(5) | 2.17(5) | 2.921(3) | 159(5) |
| C(2)–H(3)···O(8)[3] | 0.95(3) | 2.75(3) | 3.408(3) | 126(2) |
| C(2)–H(3)···O(8) | 0.95(3) | 3.05(3) | 3.676(3) | 125(2) |
| C(2)–H(3)···O(10) | 0.95(3) | 2.81(3) | 3.548(3) | 135(2) |
| C(3)–H(4) | 0.94(3) | | | |
| C(6)–H(7)···O(4)[7] | 0.99(3) | 2.45(3) | 3.353(2) | 152(2) |
| C(7)–H(8)···O(14)[8] | 0.95(3) | 2.98(3) | 3.855(3) | 154(2) |

*(Symmetry codes: (1) -x+2,y-1/2,-z+1/2; (2) x+1,y,z; (3) -x+1,y+1/2,-z+1/2; (4) -x,y-1/2,-z+1/2; (5) x,-y+1/2,z-1/2; (6) x,-y+3/2,z-1/2; (7) x-1,y,z; (8) x,-y+1/2,z+1/2.)*

in the vessel after TG-DTA measurements of L-$SrC_4H_4O_6{\cdot}4H_2O$, DL-$CaC_4H_4O_6{\cdot}4H_2O$, and DL-$SrC_4H_4O_6{\cdot}4H_2O$, and that after the evolution of gases from L-$BaC_4H_4O_6$, barium monocarbide (BaC) remains on the inside surface of the vessel, which turns black in color [4,5,13,14]. There are two types of crystallographically independent $C_4H_4O_6$ molecules in the unit cell of DL-$BaC_4H_4O_6{\cdot}H_2O$. Consequently, we consider that the white oxide and monocarbide products are each generated from one of the two $C_4H_4O_6$ molecules. The chemical reactions during the decompositions of L-$BaC_4H_4O_6$ and DL-$CaC_4H_4O_6{\cdot}4H_2O$ mentioned in the introduction allow us to assume that two reaction processes are involved in the decomposition of DL-$BaC_4H_4O_6{\cdot}H_2O$, and that these can be represented as follows:

| | | |
|---|---|---|
| 300–500 K | $2BaC_4H_4O_6{\cdot}H_2O \rightarrow 2BaC_4H_4O_6 + 2H_2O$ | |
| 500–900 K | $BaC_4H_4O_6 \rightarrow BaCO_3 + 2H_2 + 3CO$ | $BaC_4H_4O_6 \rightarrow BaC_2O_4 + 2H_2CO$ |
| 900–1080 K | $BaCO_3 \rightarrow BaCO_2 + (1/2)O_2$ | $BaC_2O_4 \rightarrow BaCO_3 + CO$ |
| 1080–1550 K | $BaCO_2 \rightarrow BaC + O_2$ | $BaCO_3 \rightarrow BaO + CO + (1/2)O_2$. |

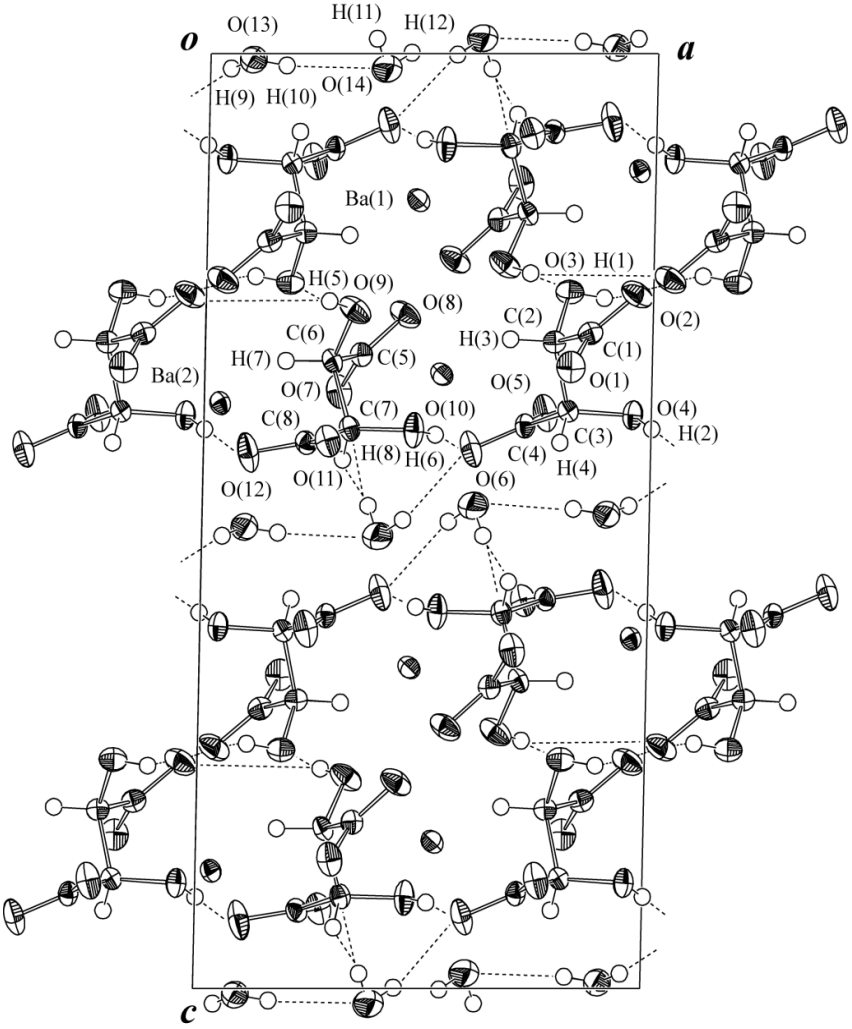


**Fig. 1. Projection of the crystal structure of DL-$BaC_4H_4O_6{\cdot}H_2O$ along the *b*-axis at room temperature with 60% probability-displacement thermal ellipsoids. The solid and dashed short lines indicate O–H···O hydrogen bonds, as shown in Table 4**

**Table 5. TG results for thermal decomposition of DL-$BaC_4H_4O_6 \cdot H_2O$**

| Temp. range [K] | Weight loss (obs.) [%] | Weight loss (cal.) [%] | Elimination molecules |
|---|---|---|---|
| 300–500 | 7.7 | 5.9 | $2H_2O$ |
| 500–900 | 25.4 | 24.4 | $2H_2 + 3CO + 2H_2CO$ |
| 900–1080 | 9.2 | 7.3 | $(1/2)O_2 + CO$ |
| 1080–1550 | 10.3 | 12.5 | $(3/2)O_2 + CO$ |
| Total | 52.6 | 50.1 | |

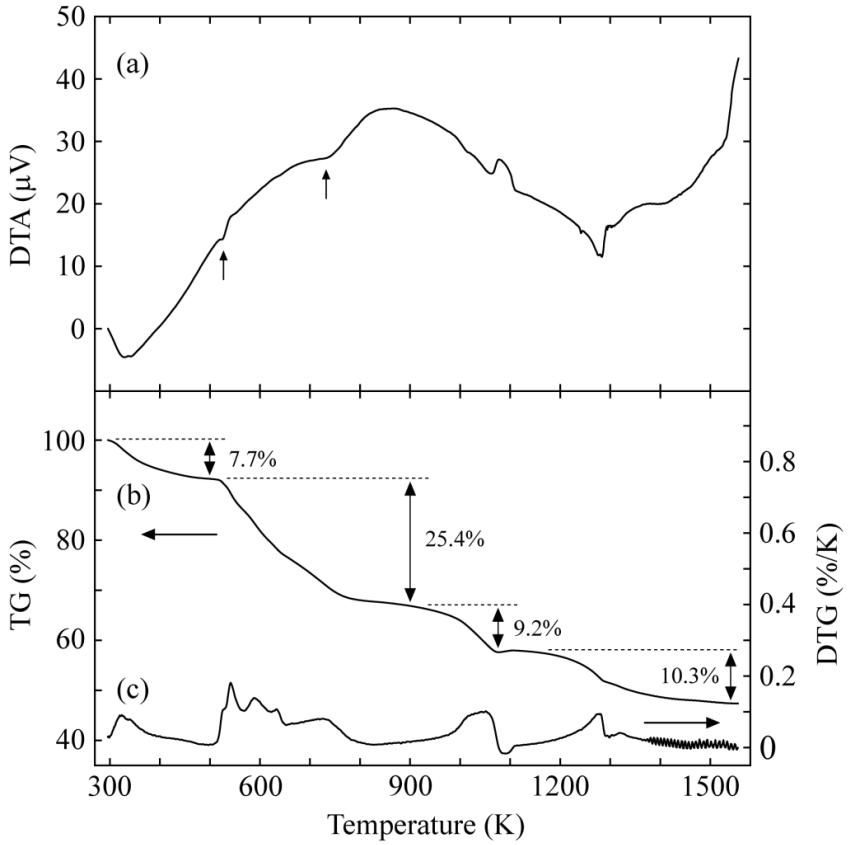


**Fig. 2. TG, DTG, and DTA thermograms for DL-$BaC_4H_4O_6 \cdot H_2O$ crystal on heating. The sample weight (powder) was 5.22 mg, and the heating rate was 10 K $min^{-1}$ under a dry $N_2$ flux of 300 ml $min^{-1}$**

The experimental weight losses obtained from the TG analysis, the theoretical losses based on the chemical reactions above, and the molecular gases eliminated at various temperature ranges are summarized in Table 5. The theoretical losses calculated for each temperature range match closely with the experimental data. However, there is a difference of 1.8% between the theoretical and experimental losses in the temperature range of 300–500 K, as shown in Table 5. In general, there are many defects in the crystal structure, such as pores and cracks, and the aqueous solution used for crystal growth can infiltrate these defects. Thus, the difference in the range of 300–500 K is probably caused by the evaporation of the infiltrated solution from these defects, and this is also the cause of the slight difference between the experimental and theoretical total losses. The other slight differences between the experimental and theoretical values at each temperature range are probably a result of overlapping temperature ranges corresponding to the decomposition reactions. The residual chalky white and black substances remaining in the vessel after heating the sample up to 1550 K are barium oxide (BaO) and BaC, respectively, as suggested by the chemical equations as described above. If

significant differences in the Ba–O or Ba–C distances exist, we can determine the corresponding relation between the evaporation products (BaO or BaC) and the two $C_4H_4O_6$ molecules. However, we could not find a relationship between the products and molecules because of the lack of the significant differences in these distances, as shown in Table 3.

## 4. SUMMARY

Single crystals of DL-$BaC_4H_4O_6{\cdot}H_2O$ have been grown in silica gel medium at 308 K by the diffusion method. The thermal properties and crystal structure of the single crystals are studied by DSC, TG-DTA, and X-ray diffraction. The room temperature crystal structure, including the positional and thermal parameters of all the hydrogen atoms, is determined to be monoclinic with space group $P2_1/c$ by means of single-crystal X-ray diffraction. We found that the structure consists of $BaO_9$ and $BaO_{10}$ polyhedra, two independent $C_4H_4O_6$ molecules, and O–H···O and C–H···O hydrogen bonds between adjacent $H_2O$ or $C_4H_4O_6$ molecules. No phase transition was observed in the temperature range of 100–322 K, and weight losses due to the thermal decomposition of DL-$BaC_4H_4O_6{\cdot}H_2O$ were found to occur in the temperature range of 300–1550 K. The chemical equations illustrating the decomposition reactions of DL-$BaC_4H_4O_6{\cdot}H_2O$ are presented with the corresponding temperature ranges. We concluded that the weight losses are caused by the evaporation of two bound water molecules and the evolution of $2H_2CO$, $2H_2$, 5CO, and $2O_2$ gases from the two independent $C_4H_4O_6$ molecules, and that the residual chalky white and black substances mixed together in the vessel after decomposition are BaO and BaC, respectively.

## COMPETING INTERESTS

Authors have declared that no competing interests exist.

## REFERENCES


1. Desai CC, Patel AH. Crystal data for ferroelectric $RbHC_4H_4O_6$ and $NH_4HC_4H_4O_6$ crystals. J Mater Sci Lett. 1988;7(4):371–373.
   Available:http://link.springer.com/article/10.1007/BF01730747
2. Bail AL, Bazin D, Daudon M, Brochot A, Robbez-Massond V, Maisonneuve V. Racemic calcium tartrate tetrahydrate [form (II)] in rat urinary stones. Acta Crystallogr. 2009;B65(3):350–354.
   Available:http://dx.doi.org/10.1107/S0108768109013688
3. Labutina ML, Marychev MO, Portnov VN, Somov NV, Chuprunov EV. Second-order nonlinear susceptibilities of the crystals of some metal tartrates. Crystallogr Rep. 2011;56(1):72–74.
   Available:http://dx.doi.org/10.1134/S1063774510061082
4. Fukami T, Tahara S, Yasuda C, Nakasone K. Crystal structure and thermal properties of $SrC_4H_4O_6{\cdot}4H_2O$ single crystals. Int Res J Pure Appl Chem. 2016;11(1):1–10.
   Available:http://dx.doi.org/10.9734/IRJPAC/2016/23674
5. Fukami T, Hiyajyo S, Tahara S, Yasuda C. Thermal properties and crystal structure of $BaC_4H_4O_6$ single crystals. Inter J Chem. 2017;9(1):30–37.
   Available:http://dx.doi.org/10.5539/ijc.v9n1p30
6. Fukami T, Tahara S, Yasuda C, Nakasone K. Structural refinements and thermal properties of L(+)-tartaric, D(–)-tartaric, and monohydrate racemic tartaric acid. Inter J Chem. 2016;8(2):9–21.
   Available:http://dx.doi.org/10.5539/ijc.v8n2p9
7. Bootsma GA, Schoone JC. Crystal structures of mesotartaric acid. Acta Crystallogr. 1967;*22*(4):522–532.
   Available:http://dx.doi.org/10.1107/S036510X67001070
8. Song QB, Teng MY, Dong Y, Ma CA, Sun J. (2S,3S)-2,3-Dihydroxy-succinic acid monohydrate. Acta Crystallogr. 2006; E62(8):o3378–o3379.
   Available:http://dx.doi.org/10.1107/S1600536806021738
9. Abdel-Kader MM, El-Kabbany F, Taha S, Abosehly AM, Tahoon KK, El-Sharkawy AA. Thermal and electrical properties of ammonium tartrate. J Phys Chem Solids. 1991;52(5):655-658.
   Available:https://doi.org/10.1016/0022-3697(91)90163-T
10. Torres ME, Peraza J, Yanes AC, López T, Stockel J, López DM, Solans X, Bocanegra E, Silgo GG. Electrical conductivity of doped and undoped calcium tartrate. J Phys Chem Solids. 2002;63(4):695–698.
    Available:http://doi.org/10.1016/S0022-3697(01)00216-5
11. Firdous A, Quasim I, Ahmad MM, Kotru PN. Dielectric and thermal studies on gel

grown strontium tartrate pentahydrate crystals. Bull Mater Sci. 2010;33(4):377–382.
Available:http://dx.doi.org/10.1007/s12034-010-0057-1

12. Silgo CG, Platas JG, Pérez CR, López T, Torres M. Barium L-tartrate. Acta Crystallogr. 1999;C55(5):740–742.
Available:http://dx.doi.org/10.1107/S0108270198016709
13. Fukami T, Hiyajyo S, Tahara S, Yasuda C. Thermal properties, crystal structure, and phase transition of racemic $CaC_4H_4O_6{\cdot}4H_2O$ single crystals. Am Chem Sci J. 2016;16(3):1–11.
Available:http://dx.doi.org/10.9734/ACSJ/2016/28258
14. Fukami T, Hiyajyo S, Tahara S, Yasuda C. Crystal structure and thermal properties of racemic $SrC_4H_4O_6{\cdot}4H_2O$ single crystals. Int Res J Pure Appl Chem. 2017;14(2):1–10.
Available:http://dx.doi.org/10.9734/IRJPAC/2017/34299
15. Burla MC, Caliandro R, Camalli M, Carrozzini B, Cascarano GL, Giacovazzo C, Mallamo M, Mazzone A, Polidori G, Spagna R. SIR2011: A new package for crystal structure determination and refinement. J Appl Crystallogr. 2012;45(2):357–361.
Available:http://dx.doi.org/10.1107/S0021889812001124
16. Sheldrick GM. Crystal structure refinement with SHELXL. Acta Crystallogr. 2015; C71(1):3–8.
Available:http://dx.doi.org/10.1107/S2053229614024218
17. Farrugia LJ. WinGX and ORTEP for Windows: An update. J Appl Crystallogr. 2012;45(4):849–854.
Available:http://dx.doi.org/10.1107/S0021889812029111



*Peer-review history:*
*The peer review history for this paper can be accessed here:*
*http://sciencedomain.org/review-history/21267*